Running title: dynein light intermediate chain mutant mouse

Behavioural and other phenotypes in a cytoplasmic dynein light intermediate chain 1 mutant mouse

Gareth T. Banks[1,*], Matilda A. Haas[5,*], Samantha Line[6], Hazel L. Shepherd[6], Mona AlQatari[7], Sammy Stewart[7], Ida Rishal[8], Amelia Philpott[9], Bernadett Kalmar[2], Anna Kuta[1], Michael Groves[3], Nicholas Parkinson[1], Abraham Acevedo-Arozena[10], Sebastian Brandner[3,4], David Bannerman[6], Linda Greensmith[2,4], Majid Hafezparast[9], Martin Koltzenburg[2,4,7], Robert Deacon[6], Mike Fainzilber[8], Elizabeth M.C. Fisher[1,4]

[1]Department of Neurodegenerative Disease, [2]Sobell Department of Motor Science and Movement Disorders, [3]Division of Neuropathology, [4]MRC Centre for Neuromuscular Diseases, UCL Institute of Neurology, Queen Square, London, WC1N 3BG, UK
[5]MRC National Institute for Medical Research, Mill Hill, London NW7 1AA, UK
[6]Department of Experimental Psychology, University of Oxford, Oxford, OX1 3UD, UK
[7]UCL Institute of Child Health, Guilford Street, London, WC1N 1EH, UK
[8]Department of Biological Chemistry, Weizmann Institute of Science, 76100 Rehovot, Israel
[9]School of Life Sciences, University of Sussex, Brighton, BN1 9QG, UK
[10]MRC Mammalian Genetics Unit, Harwell, OX11 ORD, UK

*These authors contributed equally.

Corresponding author: Elizabeth M.C. Fisher
Email: e.fisher@prion.ucl.ac.uk
Telephone: +44 207 837 3611
Fax: +44 207 676 2180

Supplementary Information

Materials and methods

Heteroduplex screening of the MRC Mammalian Genetics Unit ENU mutagenised DNA archive

Genomic DNA samples were pooled 4 into 1 well (12.5ng per individual genomic DNA, total 50ng per well) and were amplified to produce 248bp fragment that included exon 5 of *Dync1li1*: forward primer: CACATGGTTCCATTTCTAAACTG; reverse primer: GACAGTTAGTTGCAAGGTCAG. Resulting amplicons were repeatedly denatured and reannealed before screening for the presence of heteroduplex regions on a Transgenomic WAVE model 4500 (http://www.transgenomic.com/pd/items/WAVE%204500%20all.asp). One pool was identified containing a likely heteroduplex region. The four constituent genomic DNA samples were sequenced across exon 5 of *Dync1li1* using the primers shown above on an Applied Biosystems 3130xl Genetic Analyzer and one DNA sample was identified that carried a heterozygous *Dync1li1*^{N235Y} mutation.

Open field behaviour

Female mice were placed individually into one corner of an enclosed arena (gray polyvinyl chloride; 50 × 30 × 18 cm, divided into 10 × 10-cm squares), facing the side walls, and observed for 3 min. The total numbers of squares crossed, rears, and latency to first rear were recorded.

Food consumption

Female mice were housed individually with accesses to food (standard laboratory chow, PCD Mod; Special Diet Services, Witham, Essex, United Kingdom) and water *ad libitum*. Consumption of food and water was measured over a 24 hour period.

Glucose preference

Female mice were housed individually with access to food *ad libitum*, and were provided with both water and 7.5% (wt/vol) glucose solution. The bottles were weighed after 24 hours and the ratio of glucose:water consumption was calculated. The test was performed on two consecutive days.

Wheel running

Female mice were singly housed in a cage containing a running wheel (Bio-Serv Fast-Trac wheel attached to a mouse igloo) attached to a pedometer. After 24 hour the distance run, average speed and maximum speed were recorded. Testing was performed twice.

Accelerating rotarod

Female mice were placed on the rod whilst it was rotating at 4 revolutions per min (rpm). If the animal fell off the rod before 10 sec had elapsed, the test was restarted (if the animal fell three times, the test was ended and a score of 4 rpm was recorded). After 10 sec at 4 RPM, the rod began to accelerate at 20 rpm/min. The speed at which the rod was rotating when the animal fell off was recorded. If an animal held on to the rod and made a full revolution, it was considered to have fallen off, and the speed of rotation was recorded. The rotarod was built in-house and similar to the Ugo Basile model (7650).

Hippocampal spatial working memory, reference memory acquisition and reversal

Hippocampal spatial working memory was examined using a test of spontaneous alternation (**Figure S2D**). *Dync1li1*$^{N235Y/N235Y}$ female mice did not differ from wildtypes in the number of correct alternations ($t(21)=0.10$; $p=0.92$), demonstrating intact working memory in these animals. In addition *Dync1li1*$^{N235Y/N235Y}$ mice displayed normal reference memory acquisition (effect of genotype ($F<1$); genotype*time interaction ($F(9,189)=1.16$; $p=0.39$)) (**Figures S2E, F**) and reversal (effect of genotype ($F(1,21)=1.14$; $p=0.30$; genotype*time interaction ($F(4,84)=1.78$; $p=0.17$)) (**Figures S2G, H)** in the Morris watermaze.

Modified SHIRPA screen

Modified SHIRPA was performed following the protocols outlines in (Rogers et al., 1997;Rogers et al., 2001). Briefly, mice were observed in a clear cylindrical Perspex viewing jar and assessed for body posture and the presence of tremors. Mice were then transferred to an arena (55 × 33cm) and assessed for motor behavior. Mice were then assessed while suspended by the tail for hind limb clasping. A final assessment of motor behavior was then taken via wire maneuver and movements on a horizontal screen. Full details of the SHIRPA assessment can be found at http://empress.har.mrc.ac.uk/browser/?sop_id=10_002_0.

A modified SHIRPA screen was undertaken with 3 wildtype and 4 *Dync1li1*$^{N235Y/N235Y}$ males and 4 wildtype and 9 *Dync1li1*$^{N235Y/N235Y}$ females at 12, 20, 26 and 52 weeks of age (all at N2 backcrossed to C57BL/6J) (Rogers et al., 1997;Rogers et al., 2001). We found no obvious differences between wildtype and *Dync1li1*$^{N235Y/N235Y}$ homozygous mice in this screen (data not shown).

In addition grip strength, rotarod analysis and collection of body weight data were performed at monthly intervals on female wildtype and *Dync1li1*$^{N235Y/N235Y}$ mice from 2 to 8 months of age ($n\geq10$ for all time points for both homozygotes and wildtype controls; all at N2 to N4 backcrossed to C57BL/6J) (**Figure S2I**). For grip strength analysis, we found no difference between wildtype and

Dync1li1$^{N235Y/N235Y}$ mice, except at 3 months of age, at which the mutant animals showed a higher grip strength than the controls (wildtype grip strength = 5.3 ± 0.2 grams/gram; homozygote grip strength = 5.9 ± 0.2 grams/gram; p = 0.016); grip strength was normalized to body weight. On the accelerating rotarod, mutant animals performed consistently worse than wildtype animals, although this was only statistically significant in 3-month old animals (wildtype latency to fall = 124 ± 5.33 secs; homozygote latency to fall = 104 ± 6.96 secs; p = 0.003) (**Figure S2J**).

Spontaneous alternation

Spontaneous alternation was assessed in female mice in a gray, wooden, enclosed T-maze. On each trial, the mouse was placed into the start arm facing the end wall and allowed to enter a goal arm of its own choice. The mouse was confined in the chosen goal arm for 30 sec, then placed back at the beginning of the start arm and allowed a free choice of either goal arm. Whether or not the mouse alternated was recorded. Two trials were performed per day for six days.

Watermaze

Spatial reference memory was assessed female mice in an open field watermaze which consisted of a large circular tank (diameter 2.0 m, depth 0.6 m) surrounded by various prominent visual extramaze cues. The water was opacified with milk and a 10 cm escape platform was submerged 1–1.5 cm below the water surface. The swim paths of the animals were captured by a camera above the pool and specialised software ("WATERMAZE") sampled the position of the animal at 10 Hz and provided measures such as latency, pathlength, swim speed and the amount of time spent in defined regions of the pool.

Mice received four training trials per day. On each trial the mouse was placed in the pool facing the side wall from one of eight pseudorandomised starting positions. For each animal, the platform remained in a fixed location (one of two possible platform locations, which were counterbalanced across the groups). Trials ended when the mouse found the platform, or after 90 sec, at which point the animal was guided to its location by the experimenter. The mouse was then allowed to remain on the platform for 30 sec before the start of the next trial. During probe trials the platform was removed from the pool and the animals allowed to swim freely for 60 sec – the amount of time spent in each quadrant of the pool was then calculated. The acquisition experiment consisted of 10 days of training followed by a probe trial on the 11th day. The reversal experiment was performed 3 days later and consisted of two days training during which the platform in the same location as during the acquisition experiment, followed by three days training during which the platform was located in the opposite quadrant. A probe trial was performed on the 6th day.

Brain and spinal cord histology

Brains were removed and immersed in formalin for at least 16 hour at 4^{o}C. Fixed brains were mounted in paraffin and 30μm sagittal sections taken for analysis**.** Brain sections from a cohort of 3-month old animals (4 male, 4 female wildtype; 4 male, 4 female homozygous littermates; all at N3 backcrossed to C57BL/6J) and a cohort of 8-month old animals (5 wildtype, 5 homozygous littermates, females, N3) were stained with either hematoxylin and eosin (H&E) (3-months) or cresyl violet (8-months). Given the phenotypes described above particular attention was given to the prefrontal cortex, hippocampus, striatum and cerebellum but no histological differences were detected between wildtype and *Dync1li1*$^{N235Y/N235Y}$ homozygote brains (**Figure S3A**).

For spinal cord analysis, the complete spinal column was dissected, fixed in formalin for 2 days, decalcified in 0.5M EDTA for 4 days (the EDTA was changed daily) and finally fixed in formalin for one further day. The columns were mounted in paraffin and 30μm sections from the cervical, thoracic and lumbar regions taken for analysis. Spinal columns were taken from 5 wildtype and 5 homozygous littermates at 8 months of age (females, N3) and cervical and lumbar regions sections were stained with H&E. We observed no differences between wildtype and mutant animals (**Figure S3B**).

Motor neuron counts

For motor neuron survival studies, mice were perfused transcardially under terminal anaesthesia, the lumbar region of the spinal cord was removed, post-fixed and cryoprotected as described previously (Achilli et al., 2009). Serial transverse sections (20μm) examined under a light microscope (Leica DMR) using Leica HC PL Fluotar objectives (10x, 20x and 40x magnification). The number of Nissl-stained motor neurons in the sciatic motor pool of every third section (n>35) between the L3 and L6 levels of the spinal cord were counted. Only large (diameter >12μm), polygonal neurons with a distinguishable nucleus and nucleolus and clearly identifiable Nissl structure were included in the counts. Images were captured using a Nikon E995 digital camera and the images downloaded into Adobe Photoshop CS. To optimise image contrast, Levels Adjustment operations were performed, but no other image manipulations were made. Motor neuron counts were performed in the sciatic motor pool of five 12-month old *Dync1li1*$^{N235Y/N235Y}$ homozygous animals and were compared to those of 5 age-matched wildtype littermates. We found no difference between wildtype and homozygous animals (439.2 ± 23 motor neurons in wildtype animals, 418.7 ± 8.4 in homozygote animals; p = 0.44, **Figure S3C, D**).

Peripheral nerve branching during development

To assess nerve branching in developing animals we performed whole mount neurofilament immunohistochemistry in the limbs of E13.5 animals. The fore and hind limbs were dissected

from E13.5 embryos and fixed for at least 16 hour in Dent's fixative (1 part DMSO, 4 parts methanol) at 4°C. The limbs were then bleached in 1 part 30% H_2O_2; 2 parts Dent's for 2 hours, washed three times in TBS (10mM Tris-HCl pH8.0; 150mM NaCl) for 15 min each wash, washed for 30 min in blocking serum (100ml goat serum, 25ml DMSO; 0.12g thimerosal) and incubated for 16 hour in rabbit anti-Neurofilament (Chemicon) diluted 1:250 in blocking serum. The limbs were washed five times in TBS for 1 hour each wash, before washing for 16 hour in goat anti-rabbit (DAKO) diluted 1:200 in blocking serum. The limbs were again washed five times in TBS for 1 hour each wash, then washed for 30 min in FAST DAB without H_2O_2 (Sigma), washed for 1 hour in FAST DAB with H_2O_2 (Sigma), washed several times in TBS, washed for 10 min in 4%PFA in PBS, and stored in PFA at 4°C. Prior to imaging the limbs were cleared by washing in 1 part TBS: 1 part methanol, three washes in 100% methanol, and one wash in 1 part methanol: 1 part BABB (1 part benzyl alcohol: 2 parts benzyl benzoate). Finally the limbs were cleared by washing in 100% BABB until the limbs were cleared enough for adequate imaging.

The dorsal side of the limb was imaged and the number of nerve branches within the limb was counted. We found no significant difference between wildtype and *Dync1li1*$^{N235Y/N235Y}$ animals in the number of branch points in these embryos (number of branch points in the fore limb: wildtype 31.9 ± 2.0, *Dync1li1*$^{N235Y/N235Y}$ 34.1 ± 1.6; p = 0.392. Number of branch points in the hind limb: wildtype 33.6 ± 1, *Dync1li1*$^{N235Y/N235Y}$ 36.9 ± 1.6; p = 0.149. Wildtype n = 8, *Dync1li1*$^{N235Y/N235Y}$ n = 15) (**Figure S4**).

In addition wholemount neurofilament staining did not show any obvious abnormalities in the peripheral nervous system of homozygotes at P12.5 (Christiana Ruhrberg, personal communication).

Histology of the saphenous nerve

To establish whether the *Dync1li1* mutation had any effect upon the saphenous nerve itself, a histological analysis was performed upon the saphenous nerves of 3 wildtype and 3 mutant mice. We found no difference between wildtype and mutant mice in average fibre size (wildtype 4.1 ± 0.1μm, *Dync1li1*$^{N235Y/N235Y}$ 4.0 ± 0.1μm; p >0.1) (**Figure S5C**), fibre size distribution (**Figure S5D, Table S3**), g-ratio (wildtype 0.68 ± 0.003, *Dync1li1*$^{N235Y/N235Y}$ 0.68 ± 0.006; p > 0.9 1.0) (**Figure S5E**) or average axonal diameter (wildtype 2.7 ± 0.01 μm, *Dync1li1*$^{N235Y/N235Y}$ 2.7 ± 0.05 μm; p >0.5) (**Figure S5F**).

Saphenous nerve morphometry

Saphenous nerves were dissected from animals used in the skin nerve preparations described above and immersion fixed in 3% gluaraldehyde in 0.05 M sodium cacodylate buffer pH 7.4 for at

least 16 hours at 4^{o}C. Samples were processed as described previously (Achilli et al., 2009) and embedded in araldite CY212 epoxy resin. Semithin sections (0.8 µm) were cut on an Ultracut E ultra microtome (Leica) and stained with 1% toluidine blue containing 1% borax (BDH). Sections were photographed at a 40x magnification and nerve fibre measurements were taken using a Leica Quantimet image analyzer.

Neurophysiology of lumbar motor neurons

As *Dync1li1*$^{N235Y/N235Y}$ animals have a different gait from wildtype littermates, motor nerve conduction velocity was assessed in 5 wildtype and 5 *Dync1li1*$^{N235Y/N235Y}$ homozygous littermates (both sexes, 4 or 5 months of age). Compound action potentials were recorded from intrinsic foot muscles following supramaximal electrical stimulation of the sciatic or tibial nerve at the sciatic notch or ankle, respectively. We found no differences between wildtype and homozygous animals in the conduction velocity (wildtype 37.8 ± 2.4 m/s, *Dync1li1*$^{N235Y/N235Y}$ 37.2 ± 1.9 m/s; p >0.8), the distal motor latency (wildtype 1.2 ± 0.2 ms, *Dync1li1*$^{N235Y/N235Y}$ 1.2 ± 0.1 ms; p >0.8) or amplitude of the compound muscle action potential following stimulation of the tibial nerve at the ankle (wildtype 22.9 ± 3.7 mV, *Dync1li1*$^{N235Y/N235Y}$ 23.6 ± 3.9 mV; p >0.8). Needle EMG of the intrinsic foot muscles showed no spontaneous activity in form of fibrillation potentials or positive sharp waves indicating that there was no terminal degeneration of motor axons.

Cellular localization of DYNC1LI1 and RAB4 in cortical neurons

Cortical neurons from wildtype and *Dync1li1*$^{N235Y/N235Y}$ homozygote animals and were immunolabelled with our DYNC1LI1 antibody or a commercial RAB4 antibody (Santa Cruz); DYNC1LI1 and RAB4 had diffuse punctuate cytoplasmic stains in wildtype and homozygous mutant neurons, suggesting the mutation causes no gross changes in the cellular localization of these proteins (**Figure S8H to K**).

Dynein subunit levels and interactions

We generated antibodies against wildtype DYNC1LI1, and the dynein intermediate chain protein 1, DYNC1I1. The specificity of these antibodies was verified on western blots by probing homogenates of mouse brains and HEK293T cell lines expressing GFP-tagged constructs of dynein proteins (**Figures S7**). In each case the antibody detected protein bands of the correct size, which were not detected in homogenates of untransfected HEK293T cells.

To investigate if the DYNC1LI1 mutation affected its stability or expression, or its interactions with other components of the dynein complex, we assessed protein levels in brain homogenates from 12-month old wildtype and *Dync1li1*$^{N235Y/N235Y}$ mice. Quantitative western blots were probed with antibodies to the dynein subunits DYNC1LI1, DYNC1I, DYNC1I1, DYNLT1, DYNLT3, DYNLL,

and to the cargo RAB4A (**Figure S8A**) and expression levels were normalized against beta-actin (**Figure S8B** and **Table S4**). We found no differences in individual protein levels, except for a significant increase in the levels of DYNLT3 in *Dync1li1*$^{N235Y/N235Y}$ mice compared to wildtype controls (p = 0.001; **Figure S8** and **Table S4**).

We performed co-immunoprecipitation studies on brain homogenates of 12-month old wildtype and *Dync1li1*$^{N235Y/N235Y}$ mice using either a commercially available DYNC1I antibody (IC-74) or our DYNC1LI1 specific antibody. Levels of co-immunoprecipitating proteins were normalized against the levels of the protein used to pull down the complex. When the dynein complex was precipitated using the IC-74 antibody we found no difference between wildtype and homozygote samples in the levels of co-precipitating DYNC1LI1; similarly when we precipitated using our DYNC1LI1 specific antibody we found no difference between wildtype and homozygote samples in the levels of co-precipitating DYNC1I (**Figure S8C, D** and **Table S5**). Thus DYNC1LI1^{N235Y} was still bound within the complex. We then determined if the mutation had an effect upon the levels of light chains found within the intact complex: we found no difference between wildtype and homozygote samples in the levels of co-precipitating DYNLT1 or DYNLT3, however, there was a significant decrease in the amount of co-precipitating DYNLL in mutant samples when compared to wildtype (p = 0.000005; **Figure S8D** and **Table S5**).

The dynein complex has a role in autophagy (Ravikumar et al., 2005), and so we analyzed LC3 II levels in brain homogenates of 12-month old wildtype (n=4) and *Dync1li1*$^{N235Y/N235Y}$ littermates (n=4), by quantitative western hybridization: in *Dync1li1*$^{N235Y/N235Y}$ LC3 II levels were 100.8 ± 5.06% those of wildtypes (**Figure S8F, G)**, indicating autophagy is not affected by the mutation. We found no differences in cellular localization of DYNC1LI1 or its cargo RAB4 between wildtype and mutant animals in cortical neurons (Supplementary Information and **Figure S8H-K**).

Western hybridization and protein quantification

Mice were killed by cervical dislocation according to UK Home Office regulations and brains were individually weighed and homogenized immediately in PBS with protease inhibitors (10% w/v). Samples were western blotted onto PVDF membrane (ImmobilonP) as described previously (Achilli et al., 2009). Antibody hybridization was as described and the results visualised using CPD-Star (Roche); blots were stripped and reprobed using an antibody against beta-actin (Sigma A5441) (Achilli et al., 2009). Autoradiographs were quantified using Imagemaster 1D software (Amersham Pharmacia Biotech) and protein levels normalised to β-actin levels. Primary antibody concentrations used in western blotting: anti-DYNC1LI1, anti-DYNC1I (IC-74), anti-DYNC1I1 at 1:2000; anti-DYNLT1 and anti-DYNLT3 at 1:500; anti-DYNLL at 1:10000; anti-RAB4A at 1:5000; anti-beta-actin at 1:1000.

Immunoprecipitation

Tissue homogenates as described above; 50ul Trublot anti-rabbit or anti-mouse Ig IP beads (eBioscience) were added to 500ul homogenate and suspension incubated for 1 hour, 4^{o}C on a rotating shaker. The suspension was centrifuged to remove the beads, 5ul primary antibody and 50ul fresh beads were added to the homogenate. Samples were incubated overnight, 4^{o}C on a rotating shaker. Beads were collected by centrifugation and washed three times in PBS with protease inhibitors and once in PBS with 0.05% Tween 20. Beads were collected by centrifugation and bound proteins removed by the addition of SDS loading buffer. Samples were analyzed by western blotting as above.

Antibodies

Rabbit anti-Dynein light-intermediate chain antibodies were generated by Neo-MPS (San Diego, California, USA). Peptide immunogens against which these antibodies were raised were selected following using the PredictProtein program (http://www.predictprotein.org/) and the Predicted Antigenic Peptides program of MIF Bioinformatics Tools (http://bio.dfci.harvard.edu/Tools/antigenic.pl). Briefly, the epitope peptide (ITRKPASVSPTTPTSPTEG – DYNC1LI1 amino acids 502 to 520, **Figure S7A, B**) was coupled to Keyhole Limpet Hemocyanin via an n-terminal Cysteine, emulsified in complete Freund's adjuvant and injected into three rabbits. Crude antisera were taken from rabbits after 70 days and affinity purified using columns containing the immunogen peptide bound to insoluble beads (Multiple Peptide Systems); crude antiserum was mixed with Immunopure gentle Ag/Ab binding buffer (Pierce) and was allowed to flow through the column. Bound antibodies were eluted using Immunopure gentle Ag/Ab elution buffer (Pierce). Purified antibodies were dialysed against 50 mM Tris-HCl and then against PBS and concentrated using Vivaspin 500 columns.

Rabbit anti-dynein intermediate chain 1 antibodies were generated by 21st Century Biochemicals (Marlboro,Massachusetts, USA) following the same protocol. Epitope peptides were ADMQQKKEPVQDDSDL (DYNC1I1 amino acids 37 to 52) and VEPKIGHDSELENQEKKQET (DYNC1I1 amino acids 189 to 208, **Figure S7C, D**); both epitopes were injected into the same rabbit.

The following antibodies were used in western blotting and immunoprecipitation protocols: mouse anti-cytoplasmic dynein intermediate chain IC74 (Chemicon international); rabbit anti-dynein light chain LC8 (Abcam); rabbit anti-Rab4A (Santa Cruz); mouse anti-beta actin antibodies (Sigma); goat anti-mouse IgG and goat anti-rabbit IgG alkaline phosphatase conjugated secondary antibodies (Sigma); Trueblot goat anti-rabbit HRP linked secondary (Insight). IgG from rabbit

serum (Sigma) was used for non-specific binding controls in immunoprecipitation experiments. Mouse anti TCTEX1 and anti RP3 antibodies were a kind gift from Kevin Pfister (University of Virginia, (Lo et al., 2007)).

Figure S1. Mutation analysis and sequencing of *Dync1li1* amplicons
(A) WAVE heteroduplex analysis identified a possible mutation in the amplicon including exon 5 of mouse *Dync1li1*. The blue line shows the signal from the majority of samples which are wildtype, the red line, as indicated, comes from the pool of four DNAs that included the possible mutant sample.
(B) Sequencing verified the presence of an A to T mutation at base pair 754 in exon 5 of *Dync1li1* in one of the four DNA samples; the red W indicates the heterozygous AT genotype. Sequence from a subsequently bred homozygous *Dync1li1*$^{N235Y/N235Y}$ animal is shown for comparison.

Figure S2. Behaviour of *Dync1li1*$^{N235Y/N235Y}$ mice
(**A**) *Dync1li1*$^{N235Y/N235Y}$ mice did not differ from wildtypes in their consumption of food, water or a 7.5% solution of glucose over 24 hours.
(**B**) They also did not differ from wildtypes on wheel running.
(**C**) *Dync1li1*$^{N235Y/N235Y}$ mice displayed a trend towards increased strength on a test of weight lifting.
(**D**) *Dync1li1*$^{N235Y/N235Y}$ mice displayed normal spontaneous alternation on a T-maze.
(**E**) Over the course of 10 days *Dync1li1*$^{N235Y/N235Y}$ mice did not differ from wildtypes on the acquisition of a spatial reference memory task in the Morris watermaze (distance swum to reach the hidden platform was averaged over four trials per day).
(**F**) They also showed a normal preference for the target quadrant during probe test 1 (conducted on day 11).
(**G**) The pattern of behaviour of *Dync1li1*$^{N235Y/N235Y}$ mice did not differ significantly from that of wildtypes on a watermaze reversal task. The hidden platform was moved to the opposite quadrant on day 3.
(**H**) *Dync1li1*$^{N235Y/N235Y}$ and wildtype mice displayed a similar preference for the target quadrant and opposite quadrant (previously the target). AdjL = quadrant adjacent left of target; AdjR = quadrant adjacent right of target; Opp = quadrant opposite target.
(**I**) Forepaw grip strength, normalized to weight, of *Dync1li1*$^{N235Y/N235Y}$ female mice (n ≥ 10 for all time points) compared to sex-matched wildtype littermates (n ≥ 10 for all time points) from 2 to 8 months of age.
(**J**) Accelerating rotarod scores (latency to fall (s)) of *Dync1li1*$^{N235Y/N235Y}$ female mice (n ≥ 10 for all time points) compared to sex-matched wildtype littermates (n ≥ 10 for all time points) from 2 to 8 months of age.

Figure S3. Histological analysis of wildtype and *Dync1li1*$^{N235Y/N235Y}$ brain and spinal cord
(A) Haematoxylin and eosin (H&E) stained sections of brain from 3-month old wildtype and homozygous littermate controls. Representative sections of cerebellum, hippocampus, striatum and prefrontal cortex are shown. Scale bar = 200μm.
(B) H&E stained sections of spinal cord from 8-month old wildtype and homozygous littermate controls. Representative sections of cervical, thoracic and lumbar regions are shown. Scale bar = 250μm.
(**C**) Nissl-stained motor neurons in the sciatic motor pool of the spinal cord in 12-month old wildtype and *Dync1li1*$^{N235Y/N235Y}$ animals**.** Scale bar = 200μm.
(**D**) Spinal cord motor neuron counts in the sciatic motor pool of the spinal cord in 12-month old wildtype and *Dync1li1*$^{N235Y/N235Y}$ animals.

Figure S4. Central and peripheral neuron morphology
Cortical neuron dendrite morphology, *in vitro*
(A) The mean number of individual dendritic trees originating from the neuron soma.
(B) The mean number of nodes (branch points) per dendritic tree.
(C) The frequency of branch points per dendritic tree.
(D) Sholl analysis showing the number of dendrite intersections of concentric circles at increasing 10μm increments.

Whole mount neurofilament staining in E13.5 limbs.
(**E**) Whole mount neurofilament staining in embryonic limbs in wildtype and *Dync1li1*$^{N235Y/N235Y}$ littermates.
(**F**) Quantification of nerve branch points in embryonic limbs in wildtype and *Dync1li1*$^{N235Y/N235Y}$ littermates.

Figure S5. Lumbar dorsal root ganglia and saphenous nerve analysis.
(**A**) Lumbar DRG: A *Dync1li1*$^{N235Y/N235Y}$ mouse showing immunoreactivity for (a) NFH, (b) peripherin. (c) shows the merged images with a nuclear DAPI stain. Scale bar 50 μm.
(**B**) Lumbar DRG: A wildtype littermate showing immunoreactivity for (a) parvalbumin, (b) CGRP. (c) shows the merged images with a nuclear DAPI stain. Scale bar 50 μm.
(**C**) Saphenous nerve: Nerve fibre diameter comparisons of 3-month old wildtype and *Dync1li1*$^{N235Y/N235Y}$ homozygous littermates.
(**D**) Saphenous nerve: Fibre size distribution in 3-month old wildtype and *Dync1li1*$^{N235Y/N235Y}$ homozygous littermates.
(**E**) Saphenous nerve: G-ratio in 3-month old wildtype and *Dync1li1*$^{N235Y/N235Y}$ homozygous littermates.
(**F**) Saphenous nerve: Axon diameter comparisons of 3-month old wildtype and *Dync1li1*$^{N235Y/N235Y}$ homozygous littermates.

Figure S6. Dynein controlled processes in *Dync1li1*^{N235Y} mouse embryonic fibroblasts.
Golgi reassembly after disruption with nocodazole in *Dync1li1*$^{N235Y/+}$ MEFS. Golgi are shown in red, the cytoskeleton in green (α-tubulin) and nuclei in blue (DAPI). The scale bar represents 30μm. Wildtype and *Dync1li1*$^{N235Y/N235Y}$ images are the same as those shown in **Figure 6A** and are included here for comparison.

Figure S7. Generation of antibodies
DYNC1LI1
(**A**) Protein map of DYNC1LI1 showing the location of the ITRKPASVSPTTPTSPTEG peptide immunogen used to generate a DYNC1LI1 specific antibody. The red bar indicates the site of the DYNC1LI1^{N235Y} mutation. Structural information taken from (Bielli et al., 2001;Hughes et al., 1995;Tynan et al., 2000).
(**B**) Protein homogenates from mouse brain and from HEK293T cells expressing a GFP-tagged mouse DYNC1LI1 construct (M. Hafezparast, personal communication), were western blotted and probed with the DYNC1LI1 antibody. In the mouse brain a protein band is detected between 50 and 64 kDa (predicted size of DYNC1LI1 = 54.6kDa). In the transfected HEK293T cell homogenate a protein band is detected of approximately 98kDa (predicted size of construct = 88kDa). The band was not detected in untransfected cells. When the blot was stripped and re-probed with an anti-GFP antibody, only the 98kDa protein is detected, indicating that this protein is GFP-tagged. Since this is too large to simply be GFP, this protein appears to be the GFP tagged DYNC1LI1. Therefore these data suggest that this antibody is DYNC1LI1 specific.
DYNC1I1
(**C**) Protein map of DYNC1I1 showing the location of the ADMQQKKEPVQDDSDL and VEPKIGHDSELENQEKKQET peptide immunogens used to generate a DYNC1I1 specific antibody. The WD repeats domain is thought to be the dynein heavy chain binding domain; structural information taken from (Myers et al., 2007).
(**D**) Protein homogenates from mouse brain and HEK293T cells expressing GFP-tagged DYNC1I constructs (M. Hafezparast, personal communication), were western blotted and probed with the DYNC1I1 antibody. In the mouse brain a protein band is detected between 64 and 98 kDa (predicted size of DYNC1I1 ≈ 72kDa). In HEK293T cells transfected with DYNC1I1 isoforms, a protein band of just above 98kDa is detected (predicted size of construct ≈ 100kDa). The band was not detected in untransfected cells or cells transfected with DYNC1I2 constructs. This suggests that the antibody is DYNC1I1 specific.

Figure S8. Expression of cytoplasmic dynein subunits, RAB4 and LC3
Brain of wildtype and *Dync1li1*$^{N235Y/N235Y}$ mice.
(A) Western blot of cytoplasmic dynein proteins and RAB4, with the loading control beta-actin, from brain homogenates of wildtype and *Dync1li1*$^{N235Y/N235Y}$ mice**.**
(**B)** Quantification of western hybridisation results from brain homogenates comparing wildtype and *Dync1li1*$^{N235Y/N235Y}$ mice. Results are expressed as a percentage of the average density of the wildtype bands.
Quantification of immunoprecipitations.
(C) Immunoprecipitation (IP) of DYNC1I from wildtype and *Dync1li1*$^{N235Y/N235Y}$ brain homogenates. DYNC1LI1 is co-precipitated with DYNC1I. Lane 1 = wildtype IP; Lane 2 = *Dync1li1*$^{N235Y/N235Y}$ homozygote IP; Lane 3 = wildtype non-specific binding control (IP using non-specific rabbit IgG); Lane 4 = *Dync1li1*$^{N235Y/N235Y}$ non-specific binding control (IP using non-specific rabbit IgG); Lane 5 = wildtype loading homogenate; Lane 6 = *Dync1li1*$^{N235Y/N235Y}$ homozygote loading homogenate.
(**D)** Immunoprecipitation (IP) of DYNC1LI1 from wildtype and *Dync1li1*$^{N235Y/N235Y}$ brain homogenates. Other cytoplasmic dynein proteins are co-precipitated with DYNC1LI1. Lanes are the same for (A) above. Note: the co-precipitation of both DYNLT1 and DYNLT3 also detected a non-specific protein slightly larger than the target protein; in both cases we were able to establish which of the two bands was the dynein protein by comparing the band sizes to that of the single bands detected in the loading homogenate lanes. The identity of the non-specific bands detected in these gels is unknown. In the case of blots detecting DYNLT1, the non-specific band also appeared in the non-specific binding control, suggesting that the protein was bound to the immunoprecipitation beads in a non-specific manor.
(E) Quantification of co-precipitated proteins. Results are expressed as a percentage of the average density of the wildtype bands.
LC3 quantification
(F) Western hybridisation of LC3 in wildtype and *Dync1li1*$^{N235Y/N235Y}$ brains. β-actin is used as a loading control.
(G) Quantification of LC3 II comparing wildtype and *Dync1li1*$^{N235Y/N235Y}$ mice. Results are given as a percentage of the average wildtype band density.
Immunostaining of DYNC1LI1 and its interacting protein RAB4 in cultured cortical neurons.
(H) DYNC1LI1 immunolabelling (red) was punctate and confined to the cytoplasm in wildtype neurons, *in vitro*.
(I) DYNC1LI1 immunolabelling (red) was indistinguishable from wildtype neurons, in both localization and amount, in *Dync1li1*$^{N235Y/N235Y}$ mutant cortical neurons.
(J) RAB4 (red) in wildtype cortical neurons.
(K)RAB4 (red) immunolabelling in *Dync1li1*$^{N235Y/N235Y}$ mutant cortical neurons was similar to wildtype neurons.

Table S1. Percentages of NFH and peripherin immunoreactive cells in the cervical and lumbar DRG of wildtype and *Dync1li1*$^{N235Y/N235Y}$ mice; (values are mean±SEM).

	Cervical		**Lumbar**	
	Wildtype (n=3)	***Dync1li1*$^{N235Y/N235Y}$ (n=4)**	**Wildtype (n=3)**	***Dync1li1*$^{N235Y/N235Y}$ (n=4)**
Total cell profiles counted	1133	1573	1100	1472
Percentage NFH positive cells	33 ± 1 (31-34)	33 ± 3 (26-40)	33 ± 3 (28-39)	34 ± 0 (33-35)
Percentage peripherin positive cells	45 ± 7 (32-55)	46 ± 3 (38-53)	52 ± 6 (46-63)	57 ± 2 (53-63)
Percentage NFH and peripherin positive cells	5 ± 1 (3-8)	6 ± 2 (3-11)	7 ± 2 (4-11)	5 ± 1 (3-7)

Table S2. Percentages of CGRP and parvalbumin immunoreactive cells in the cervical and lumbar DRG of wildtype and *Dync1li1*$^{N235Y/N235Y}$ mice; (values are mean±SEM).

	Cervical		**Lumbar**	
	Wildtype (n=3)	***Dync1li1*$^{N235Y/N235Y}$ (n=4)**	**Wildtype (n=3)**	***Dync1li1*$^{N235Y/N235Y}$ (n=3)**
Total cell profiles counted	1184	1603	1142	1470
Percentage CGRP positive cells	20 ± 1 (19-22)	20 ± 1 (18-24)	23 ± 1 (21-25)	27 ± 3 (21-31)
Percentage parvalbumin positive cells	23 ± 4 (17-32)	18 ± 4 (9-29)	21 ± 3 (16-26)	24 ± 5 (15-32)
Percentage CGRP and parvalbumin positive cells	3 ± 1 (2-4)	3 ± 1 (1-6)	4 ± 1 (3-6)	7 ± 3 (1-10)

Table S3. Fibre size distribution in the saphenous nerves of 3-month old wildtype and

***Dync1li1*$^{N235Y/N235Y}$ mice (Figure S5D)**

	Proportion of nerve fibres							
	1-2 microns	**2-3 microns**	**3-4 microns**	**4-5 microns**	**5-6 microns**	**6-7 microns**	**7-8 microns**	**8-9 microns**
Wildtype	2.8% ± 0.78	26.4% ± 1.02	18.9% ± 1.66	22.2% ± 1.62	18.9% ± 0.68	8.3% ± 0.61	2.4% ± 1.42	0.08% ± 0.08
***Dync1li1*$^{N235Y/N235Y}$**	3.5% ± 0.84	28.9% ± 0.54	19.7% ± 0.95	21.9% ± 0.51	18.4% ± 1.83	6.13% ± 1.27	1.27% ± 0.13	0.1% ± 0.1
***p* value**	0.57	0.11	0.72	0.88	0.81	0.1	0.5	0.9

Table S4. Protein quantification in whole brain of 12-month old wildtype and *Dync1li1*$^{N235Y/N235Y}$ homozygous mice.

	Band density as a percentage of average wildtype band density				
	Wildtype	***Dync1li1*$^{N235Y/N235}$**	***p* value**	**n**	**No of replicate gels**
Protein					
DYNC1LI1	100 ± 2.79	100.71 ± 5.15	0.903	4	4
DYNC1I	100 ± 3.85	103.84 ± 6.6	0.62	4	3
DYNC1I1	100 ± 4.23	91.87 ± 6.33	0.296	4	4
DYNLT1	100 ± 6.93	111.60 ± 5.42	0.21	4	3
DYNLT3	**100 ± 5.6**	**177.45 ± 19.02**	**0.0018**	4	3
DYNLL	100 ± 2.04	94.89 ± 2.81	0.166	4	2
RAB4	100 ± 4.82	109.13 ± 7.11	0.301	4	3

Table S5. Quantification of immunoprecipitated proteins from whole brain of 12-month old wildtype and *Dync1li1*$^{N235Y/N235}$ homozygous mice.

		Band density as a percentage of average wildtype band density				
		Wildtype	***Dync1li1*$^{N235Y/N235Y}$**	***p* value**	**n**	**No of replicate gels**
Immunoprecipitated protein	**Co-immunoprecipitated protein**					
DYNC1I	**DYNC1LI1**	100 ± 4.95	100.12 ± 5.43	0.986	4	2
DYNC1LI1	**DYNC1I**	100 ± 10.54	91.19 ± 5.28	0.478	4	2
	DYNC1I1	100 ± 2.15	91.08 ± 6.25	0.211	4	2
	DYNLT1	100 ± 3.77	101.48 ± 11.63	0.908	4	2
	DYNLT3	100 ± 3.59	97.88 ± 5.32	0.746	4	3
	DYNLL	**100 ± 4.79**	**67.35 ± 2.33**	**0.000005**	4	4

Reference List

Achilli F, et al. (2009) A novel mouse model with a point mutation in glycyl-tRNA synthetase (*Gars*) has sensory and motor phenotypes and profoundly reduced enzyme activity in homozygotes. Dis Mod Mech 2:359-373.

Bielli A, Thornqvist PO, Hendrick AG, Finn R, Fitzgerald K, McCaffrey MW (2001) The small GTPase Rab4A interacts with the central region of cytoplasmic dynein light intermediate chain-1. Biochem Biophys Res Commun 281:1141-1153.

Hughes SM, Vaughan KT, Herskovits JS, Vallee RB (1995) Molecular analysis of a cytoplasmic dynein light intermediate chain reveals homology to a family of ATPases. J Cell Sci 108:17-24.

Lo KW, Kogoy JM, Rasoul BA, King SM, Pfister KK (2007) Interaction of the DYNLT (TCTEX1/RP3) light chains and the intermediate chains reveals novel intersubunit regulation during assembly of the dynein complex. J Biol Chem 282:36871-36878.

Myers KR, Lo KW, Lye RJ, Kogoy JM, Soura V, Hafezparast M, Pfister KK (2007) Intermediate chain subunit as a probe for cytoplasmic dynein function: biochemical analyses and live cell imaging in PC12 cells. J Neurosci Res 85:2640-2647.

Ravikumar B, Acevedo-Arozena A, Imarisio S, Berger Z, Vacher C, O'Kane CJ, Brown SD, Rubinsztein DC (2005) Dynein mutations impair autophagic clearance of aggregate-prone proteins. Nat Genet 37:771-776.

Rogers DC, Fisher EM, Brown SD, Peters J, Hunter AJ, Martin JE (1997) Behavioral and functional analysis of mouse phenotype: SHIRPA, a proposed protocol for comprehensive phenotype assessment. Mamm Genome 8:711-713.

Rogers DC, Peters J, Martin JE, Ball S, Nicholson SJ, Witherden AS, Hafezparast M, Latcham J, Robinson TL, Quilter CA, Fisher EM (2001) SHIRPA, a protocol for behavioral assessment: validation for longitudinal study of neurological dysfunction in mice. Neurosci Lett 306:89-92.

Tynan SH, Purohit A, Doxsey SJ, Vallee RB (2000) Light intermediate chain 1 defines a functional subfraction of cytoplasmic dynein which binds to pericentrin. J Biol Chem 275:32763-32768.

Figure S1

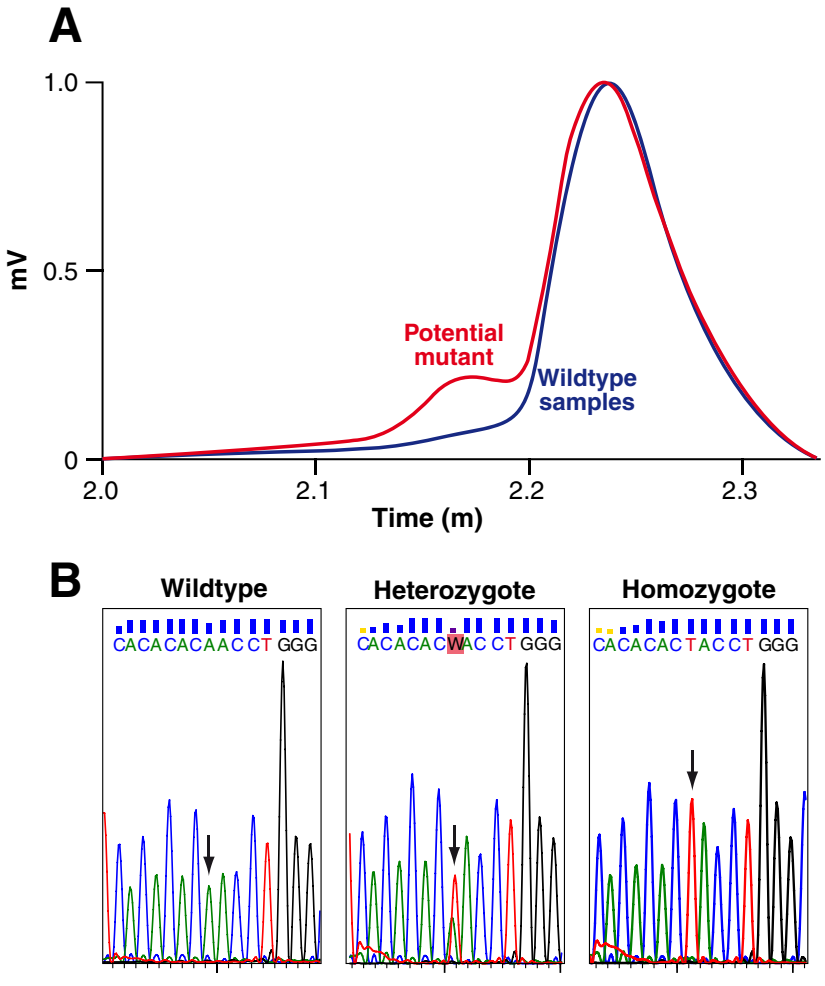
A
1.0
0.5
0
mV
Potential mutant
Wildtype samples
2.0
2.1
2.2
2.3
Time (m)
B
Wildtype
Heterozygote
Homozygote
CACACACAACCT GGG
CACACACWACCT GGG
CACACACTACCT GGG

Figure S2

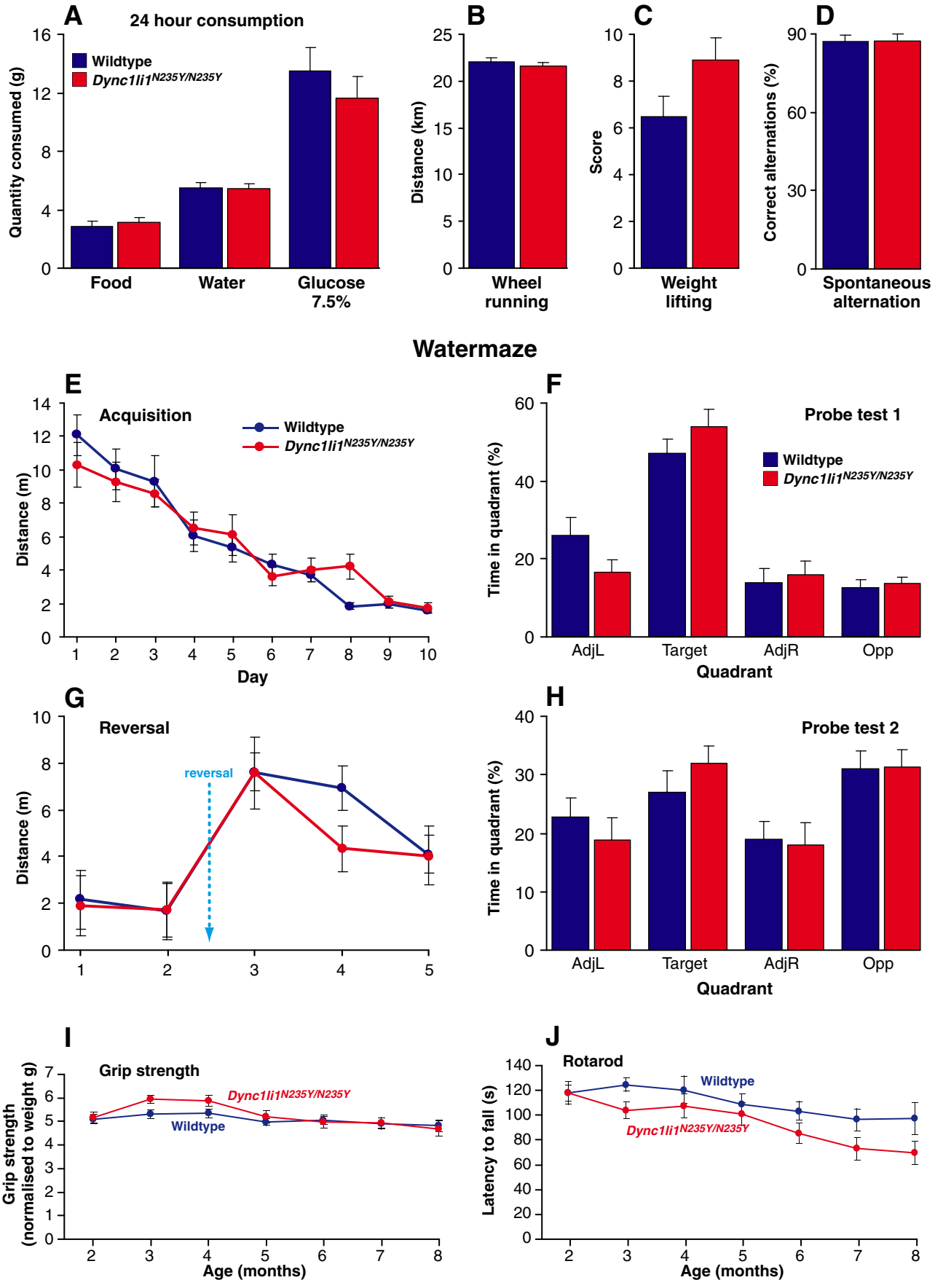
A
24 hour consumption
Wildtype
Dync1li1N235Y/N235Y
Quantity consumed (g)
Food
Water
Glucose 7.5%
B
Distance (km)
Wheel running
C
Score
Weight lifting
D
Correct alternations (%)
Spontaneous alternation
Watermaze
E
Acquisition
Distance (m)
Day
F
Probe test 1
Time in quadrant (%)
AdjL
Target
AdjR
Opp
Quadrant
G
Reversal
reversal
H
Probe test 2
I
Grip strength
Grip strength (normalised to weight g)
Age (months)
J
Rotarod
Latency to fall (s)

Figure S3

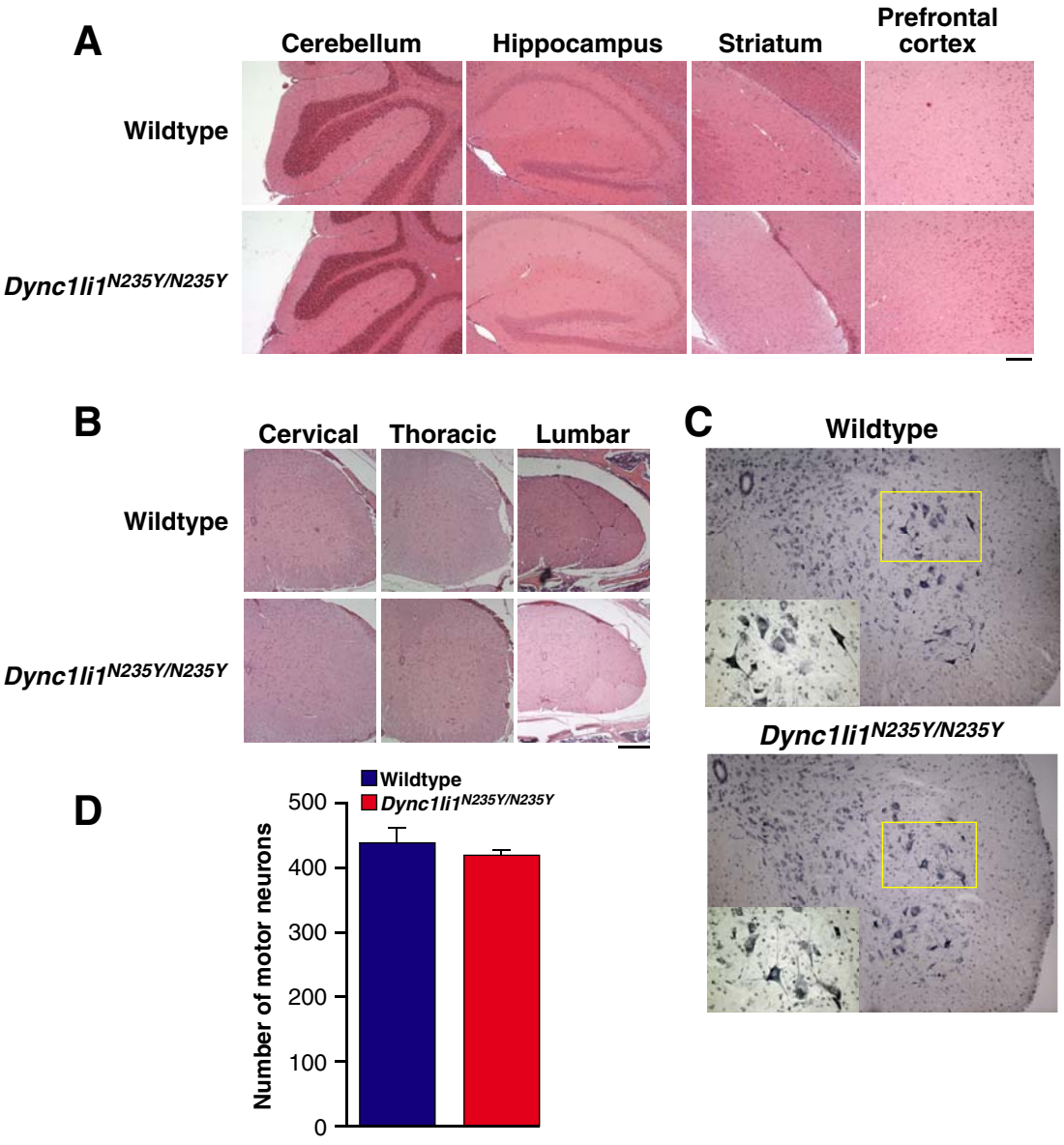
A
Cerebellum
Hippocampus
Striatum
Prefrontal cortex
Wildtype
Dync1li1N235Y/N235Y
B
Cervical
Thoracic
Lumbar
Wildtype
Dync1li1N235Y/N235Y
C
Wildtype
Dync1li1N235Y/N235Y
D
Wildtype
Dync1li1N235Y/N235Y
Number of motor neurons
500
400
300
200
100
0

Figure S4

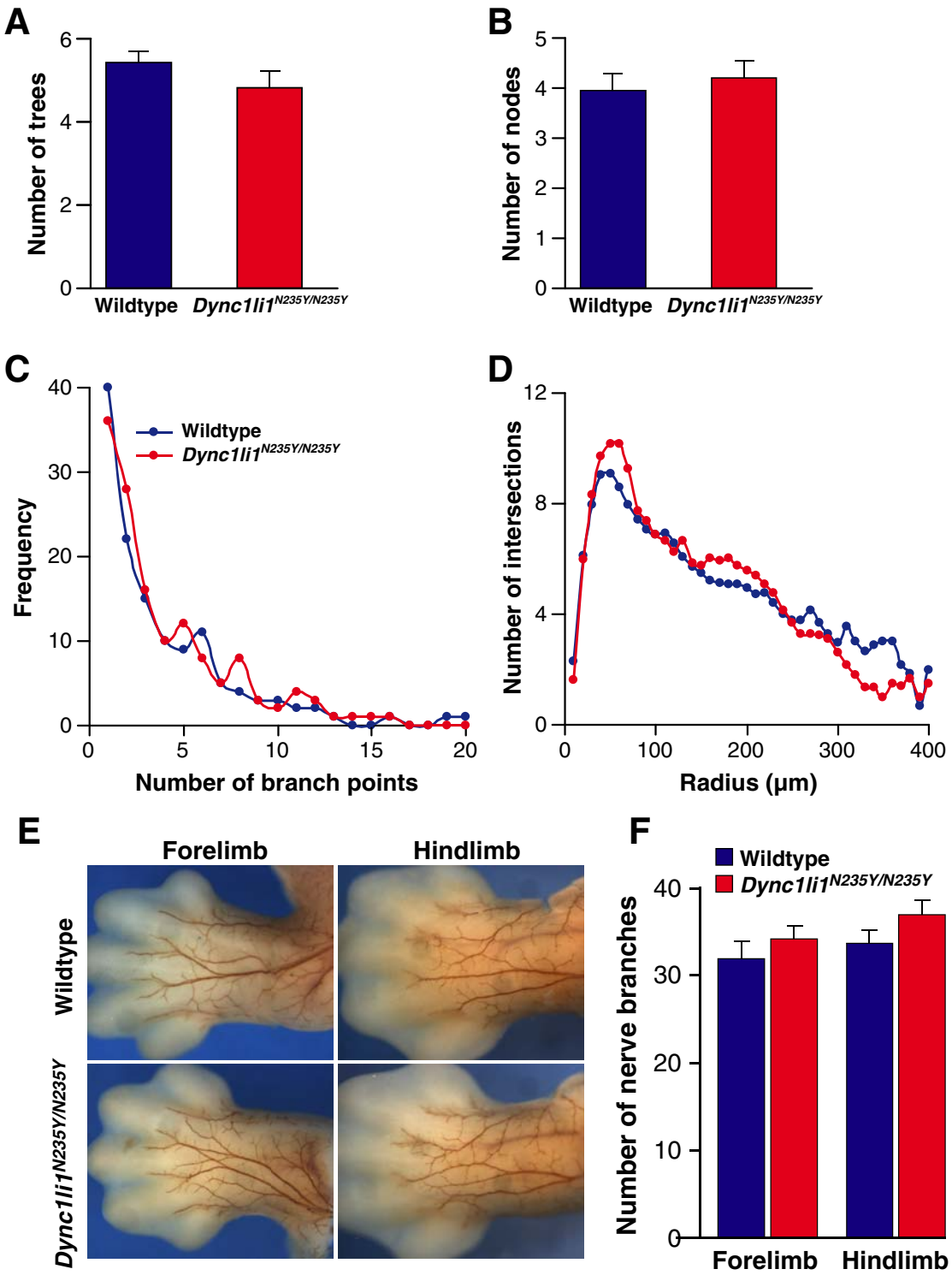
A
Number of trees
6
4
2
0
Wildtype
Dync1li1N235Y/N235Y
B
Number of nodes
5
4
3
2
1
0
Wildtype
Dync1li1N235Y/N235Y
C
Frequency
40
30
20
10
0
Wildtype
Dync1li1N235Y/N235Y
0
5
10
15
20
Number of branch points
D
Number of intersections
12
8
4
0
0
100
200
300
400
Radius (μm)
E
Forelimb
Hindlimb
Wildtype
Dync1li1N235Y/N235Y
F
Wildtype
Dync1li1N235Y/N235Y
Number of nerve branches
40
30
20
10
0
Forelimb
Hindlimb

Figure S5

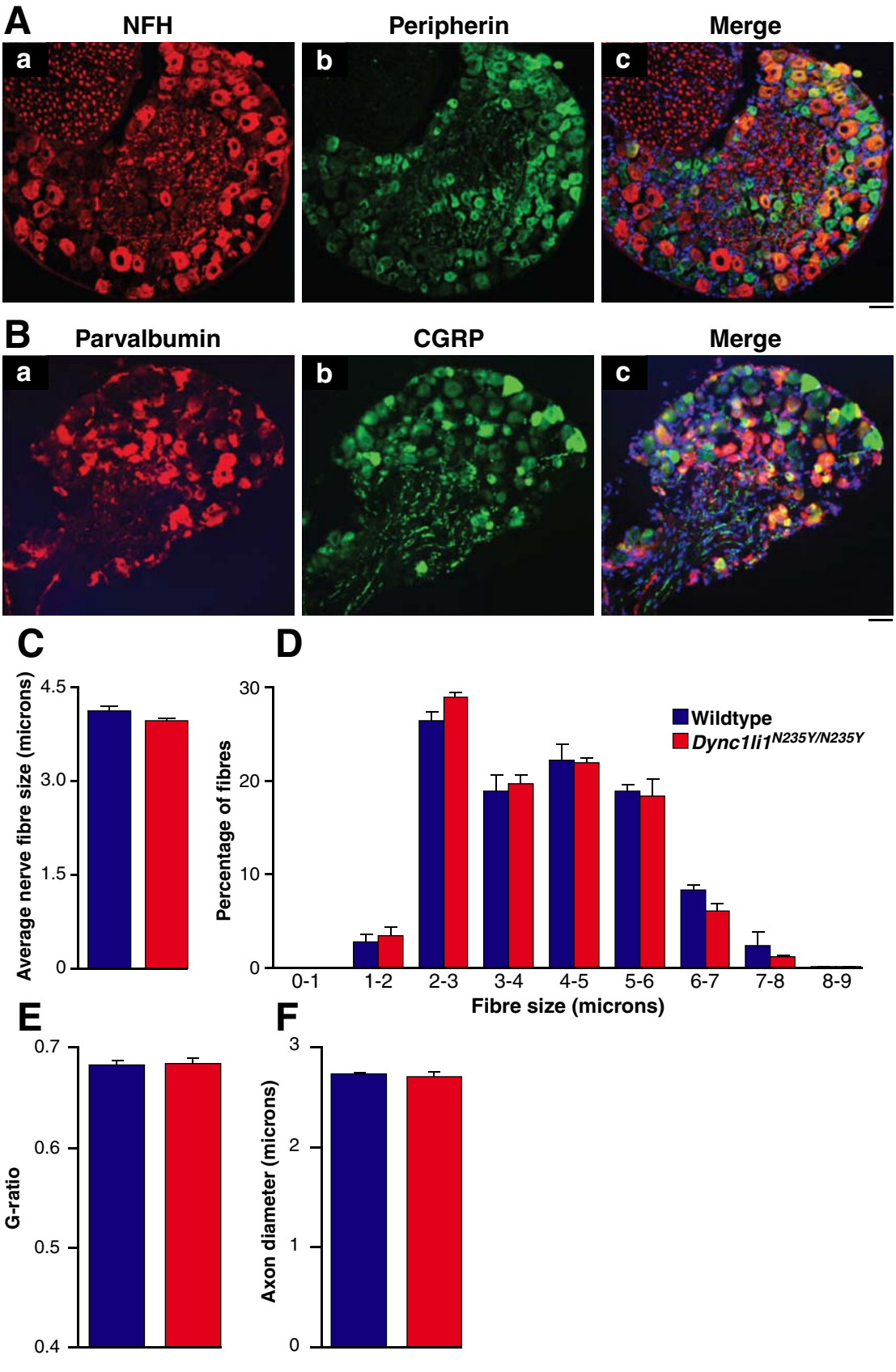
A
NFH
Peripherin
Merge
a
b
c
B
Parvalbumin
CGRP
Merge
a
b
c
C
Average nerve fibre size (microns)
4.5
3.0
1.5
0
D
Percentage of fibres
30
20
10
0
Wildtype
Dync1li1N235Y/N235Y
0-1
1-2
2-3
3-4
4-5
5-6
6-7
7-8
8-9
Fibre size (microns)
E
G-ratio
0.7
0.6
0.5
0.4
F
Axon diameter (microns)
3
2
1
0

Figure S6

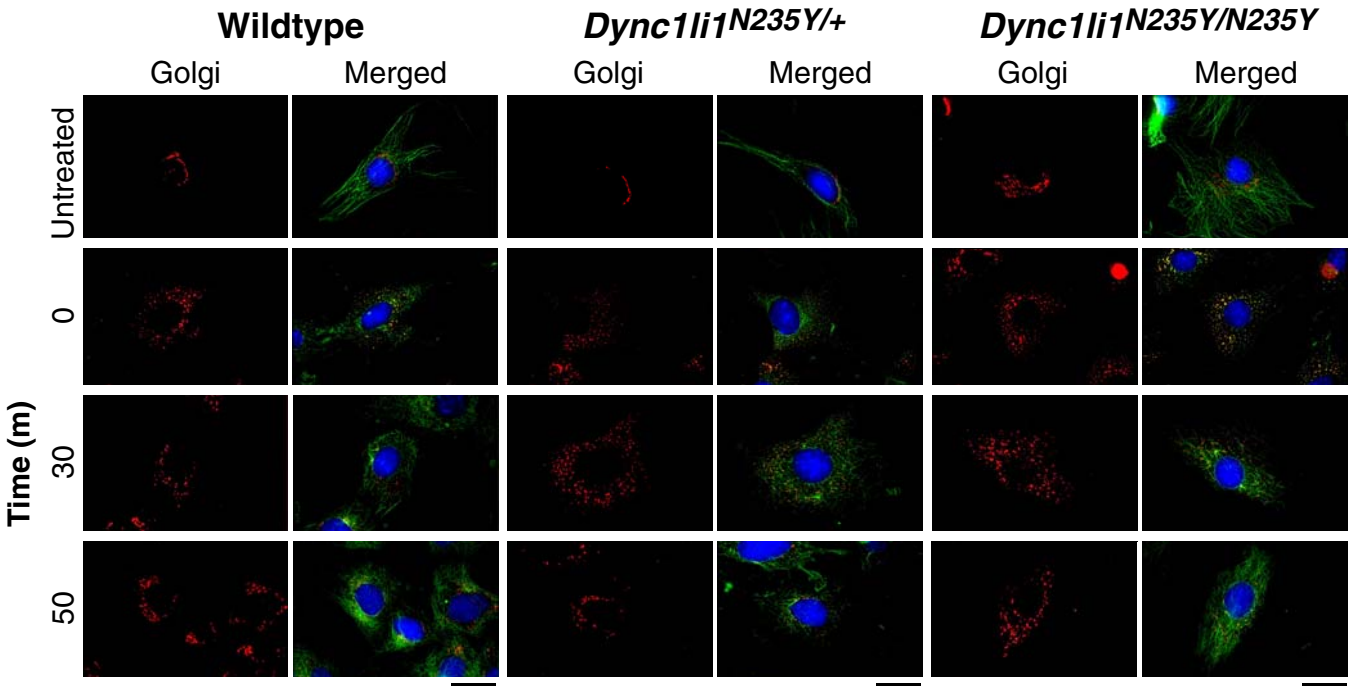
Wildtype
Dync1li1N235Y/+
Dync1li1N235Y/N235Y
Golgi
Merged
Golgi
Merged
Golgi
Merged
Time (m)
Untreated
0
30
50

Figure S7

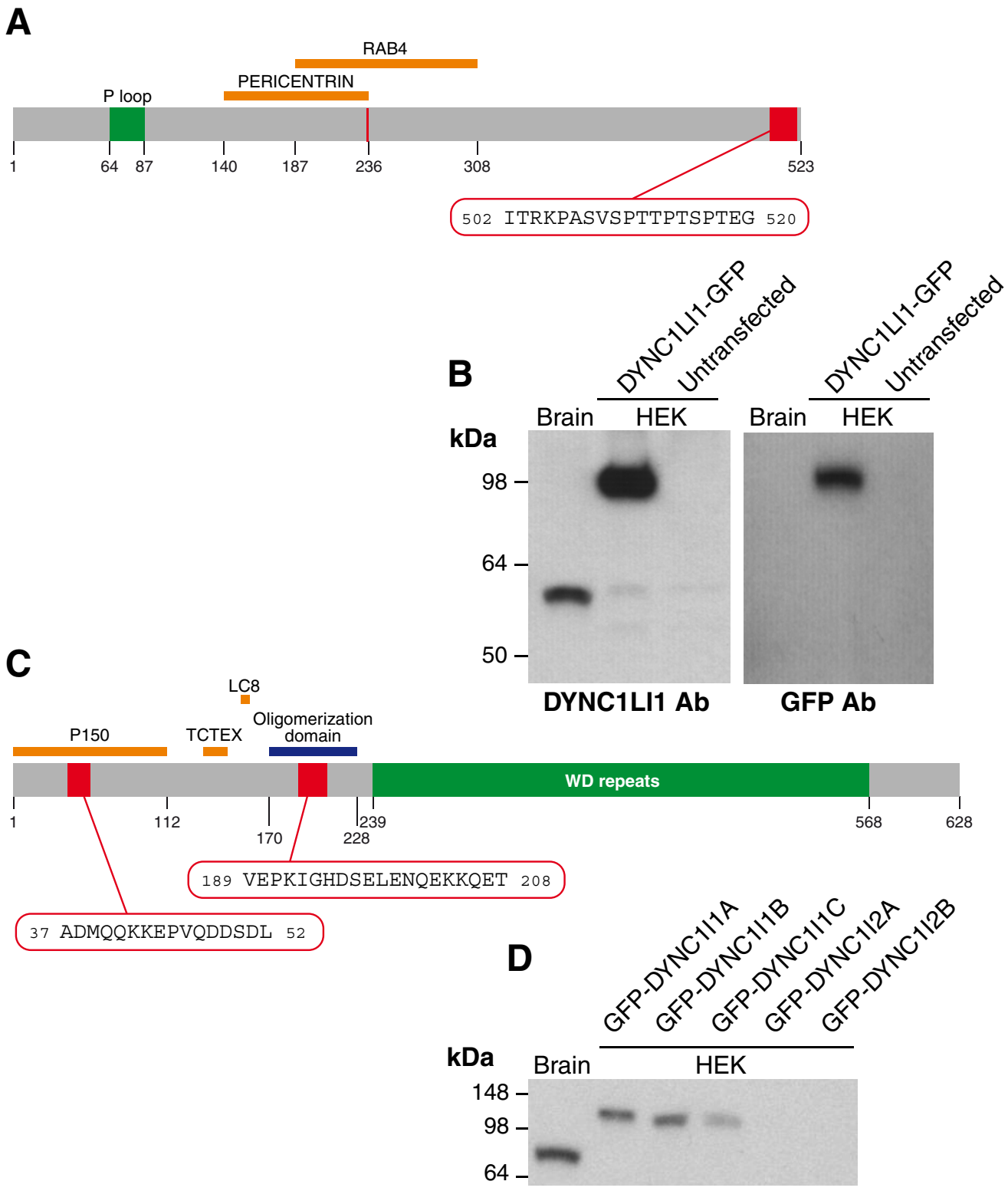
A
RAB4
PERICENTRIN
P loop
1
64
87
140
187
236
308
523
502 ITRKPASVSPTTPTSPTEG 520
B
DYNC1LI1-GFP
Untransfected
DYNC1LI1-GFP
Untransfected
Brain
HEK
Brain
HEK
kDa
98
64
50
DYNC1LI1 Ab
GFP Ab
C
LC8
P150
TCTEX
Oligomerization domain
WD repeats
1
112
170
228
239
568
628
189 VEPKIGHDSELENQEKKQET 208
37 ADMQQKKEPVQDDSDL 52
D
GFP-DYNC1I1A
GFP-DYNC1I1B
GFP-DYNC1I1C
GFP-DYNC1I2A
GFP-DYNC1I2B
kDa
Brain
HEK
148
98
64

Figure S8

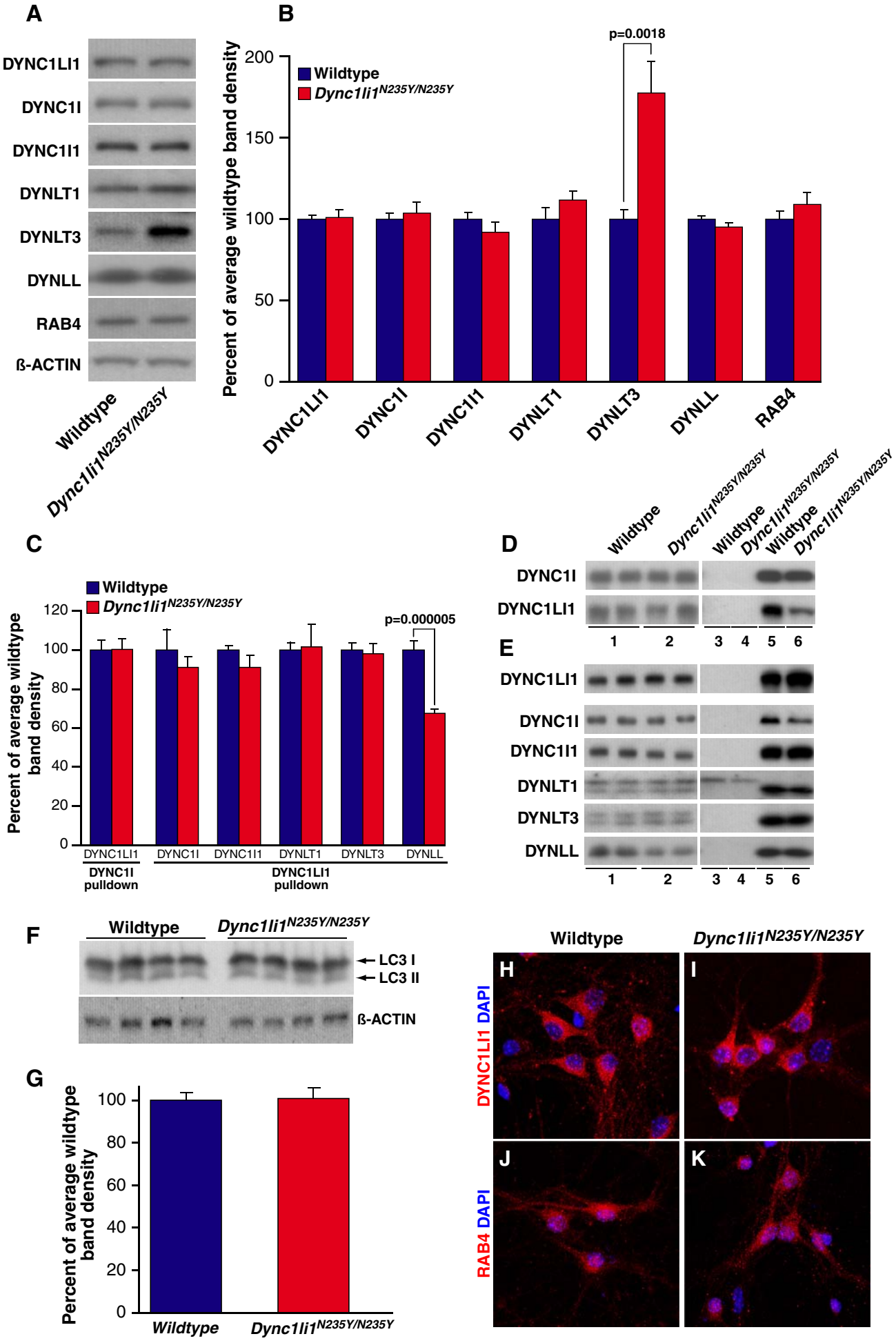
A
DYNC1LI1
DYNC1I
DYNC1I1
DYNLT1
DYNLT3
DYNLL
RAB4
ß-ACTIN
Wildtype
Dync1li1N235Y/N235Y
B
Percent of average wildtype band density
Wildtype
Dync1li1N235Y/N235Y
p=0.0018
DYNC1LI1
DYNC1I
DYNC1I1
DYNLT1
DYNLT3
DYNLL
RAB4
C
Wildtype
Dync1li1N235Y/N235Y
p=0.000005
Percent of average wildtype band density
DYNC1I pulldown
DYNC1LI1 pulldown
D
E
F
LC3 I
LC3 II
ß-ACTIN
G
Percent of average wildtype band density
H
I
J
K
DYNC1LI1 DAPI
RAB4 DAPI